AGU PUBLICATIONS

Geophysical Research Letters

RESEARCH LETTER
10.1002/2014GL061623

Key Points:
- A comprehensive assessment of WRF model parameter sensitivity is done
- Eight out of 23 parameters stand out as more sensitive than others
- The sensitive parameter list does not change with storm types, but ranks do

Supporting Information:
- Readme
- Figure S1
- Figure S2
- Figure S3
- Table S1

Correspondence to:
Z. Di,
zhdi@bnu.edu.cn

Citation:
Di, Z., Q. Duan, W. Gong, C. Wang, Y. Gan, J. Quan, J. Li, C. Miao, A. Ye, and C. Tong (2015), Assessing WRF model parameter sensitivity: A case study with 5 day summer precipitation forecasting in the Greater Beijing Area, *Geophys. Res. Lett.*, *42*, 579–587, doi:10.1002/2014GL061623.

Received 21 AUG 2014
Accepted 30 SEP 2014
Accepted article online 1 OCT 2014
Published online 22 JAN 2015

Assessing WRF model parameter sensitivity: A case study with 5 day summer precipitation forecasting in the Greater Beijing Area

Zhenhua Di[1,2], Qingyun Duan[1], Wei Gong[1], Chen Wang[1,3], Yanjun Gan[1], Jiping Quan[1], Jianduo Li[1], Chiyuan Miao[1], Aizhong Ye[1], and Charles Tong[3]

[1]College of Global Change and Earth System Science, Beijing Normal University, Beijing, China, [2]State Key Laboratory of Numerical Modeling for Atmospheric Sciences and Geophysical Fluid Dynamics, Institute of Atmospheric Physics, Chinese Academy of Sciences, Beijing, China, [3]Lawrence Livermore National Laboratory, Livermore, California, USA

Abstract A global sensitivity analysis method was used to identify the parameters of the Weather Research and Forecasting (WRF) model that exert the most influence on precipitation forecasting. Twenty-three adjustable parameters were selected from seven physical components of the WRF model. The sensitivity was evaluated based on skill scores calculated over nine 5 day precipitation forecasts during the summer seasons from 2008 to 2010 in the Greater Beijing Area in China. We found that eight parameters are more sensitive than others. Storm type seems to have no impact on the list of sensitive parameters but does influence the degree of sensitivity. We also examined the physical interpretation of parameter sensitivity. This analysis is useful for further optimization of the WRF model parameters to improve precipitation forecasting.

1. Introduction

Mesoscale numerical weather prediction models have become indispensible tools for predicting regional weather events, especially the extreme events. Over recent years, significant advancements have been achieved with better dynamical representations of the atmospheric system, higher spatiotemporal resolutions, and longer forecasting lead times [*Tripoli and Cotton*, 1982; *Dudhia*, 1993; *Janjic*, 1994; *Grell et al.*, 1995] but also in more advanced analysis methodologies such as data assimilation and model output analysis methods [*Evensen*, 1997; *Kalnay*, 2003; *Rabier*, 2005; *Wang et al.*, 2008]. The emergence of the Weather Research and Forecasting (WRF) model in the last 15 years symbolized a new era in mesoscale model development, as it is designed with a modular structure which allows easy integration of model parts developed by different groups [*Dudhia*, 2014].

The ability of the WRF model to simulate or predict weather events depends on three factors. The first factor is the realism of model physics representation. WRF, a fully compressible nonhydrostatic model with governing equations established based on physical laws, is solved on a gridded domain with spatial resolutions ranging hundreds of meters to tens of kilometers. Even with today's powerful supercomputers, it is impossible to represent many physical processes explicitly and parameterization schemes are therefore used. WRF offers a myriad of state-of-the-art physical parameterization schemes [*Skamarock et al.*, 2008]. Many studies have investigated the suitability of different schemes for simulating different physical processes [*Ruiz et al.*, 2007; *Gilliam and Pleim*, 2010; *Kim et al.*, 2011; *Nasrollahi et al.*, 2012; *Liang et al.*, 2012].

The second factor affecting WRF model performance is the specification of the initial and lateral boundary conditions. WRF has a built-in data assimilation component with alternative schemes available, including three- and four-dimensional variational data assimilations (3DVAR/4DVAR), Ensemble Transformed Kalman Filter (ETKF), and hybrid ETKF-3DVAR [*Wang et al.*, 2008; *Huang et al.*, 2009]. The data assimilation system allows WRF to ingest a vast array of observational data from diverse sources to improve the representation of initial and boundary conditions and plays a critical role in enhancing model forecasting [*Xiao and Sun*, 2007; *Liu et al.*, 2013].

The third factor impacting WRF model performance is the specification of model parameters. The WRF model contains many input parameters (i.e., constants and exponents in model equations), with some of them listed in a "namelist" file, and others hard coded in different parameterization schemes inside the computer code. The default values for them are generally assigned based on theoretical or empirical considerations by scheme developers. Some parameters may have been loosely calibrated on a limited trial-and-error basis [*Hong et al*., 2004]. How model parameters are specified has great impact on simulation of different physical processes [*Hou et al*., 2012; *Yang et al*., 2012]. Many researchers experimented with different parameter specifications to understand how they affect the simulation of a particular process. For example, *Bernardet et al*. [2000] found that good representation of topographical features, soil moisture distribution over the land, and dynamic initialization of clouds have substantial impact on how convective storm events are simulated. However, those "ad hoc" efforts to understand parametric uncertainty tend to focus on a particular scheme and are nonsystematic.

More recently, efficient and robust system-mathematical approach to parametric uncertainty analysis have become popular, which usually involves two steps: (1) identifying the parameters that have the most influence on model output and (2) tuning these parameters so model performance is optimized. Sensitivity analysis (SA) is a commonly used approach to identify the most important parameters in a model [*Saltelli et al*., 2004]. There are numerous SA studies on parameters of land surface models [*Liu et al*., 2004; *Bastidas et al*., 2006; *Hou et al*., 2012; *Li et al*., 2013]. More recently, the weather and climate modeling community is also exploring parametric uncertainty using SA methods [*Bellprat et al*., 2012; *Johannesson et al*., 2014]. Numerous studies have examined WRF parametric uncertainty with respect to precipitation forecasting [*Hong et al*., 2006; *Xiong et al*., 2010; *Yang et al*., 2012]. However, these studies were usually focused on parameters from a particular scheme. There is no comprehensive analysis of parametric uncertainty of all WRF physical schemes.

Our work intends to systematically analyze the sensitivity of all parameters that may affect precipitation forecasting in the WRF model. Our paper is organized as follows. Section 2 presents the methodology. Section 3 describes the experimental design and data used. Section 4 provides the results and discussion. Section 5 presents conclusions.

2. Methodology

There are several major steps involved in SA: (1) model and parameter selection; (2) determination of parameter uncertainty range and distribution; and (3) selection of a SA method to assess parameter sensitivity. Since our goal is to identify the most sensitive WRF model parameters for simulating precipitation, we started with selecting all parameters that may exert influence on precipitation simulation. Then we determined their uncertainty ranges and distributions by examining the physical meanings and also by consulting the WRF experts (e.g., planetary boundary layer (PBL): Songyou Hong, rapid radiative transfer model (RRTM): Eli J. Mlawer, WRF Single-Moment 6-Class Microphysics Scheme (WSM6): Jimy Dudhia). Next we chose a SA method and performed SA on the selected parameters. Section 3 presents the details on the selection of parameters, uncertainty ranges, and distributions. Here a brief description of the SA method is given.

We choose the Morris one-at-a-time (MOAT) method as the SA method for identifying the most sensitive parameters [*Morris*, 1991; *Tong*, 2005]. The MOAT method varies the value of one input variable at a time, with the other input variables remaining unchanged. It is regarded as a global sensitivity analysis method because a MOAT path spans a large portion of the input space, and the repetition of the MOAT procedure adds sampling uniformity in input space. The specific sampling procedure is as follows:

Considering one model with m-dimensional inputs $X = (x_1, x_2, \ldots, x_m)$, the ranges of each input $x_i (i = 1,2,\ldots,m)$ are normalized to [0,1]. For a given initial sample $X^0 = (x_1^0, x_2^0, \ldots, x_m^0)$, each element of which is randomly selected from the set $\{0, 1/(p-1), 2/(p-1), \ldots, 1\}$, where p is a preselected integer level (set to 4 in this study). We first randomly select the jth variable for perturbation, i.e., $X^1 = (x_1^0, \ldots, x_j^0 + \Delta_j, \ldots, x_m^0)$ and then compute the gradient of the jth variable, d_j:

$$d_j^{(1)} = \frac{f\left(x_1^0, \ldots, x_j^0 + \Delta_j, \ldots, x_m^0\right) - f\left(x_1^0, \ldots, x_j^0, \ldots, x_m^0\right)}{\Delta_j}, \tag{1}$$

where f is the cost function measuring the closeness of model simulation and observation. Δ_j is a preselected multiple of $1/(p-1)$ with a positive or a negative sign, depending on the direction of the perturbation. Then, we randomly select the second variable x_k $(k \neq j)$. We perturb x_k^0 in X^1 by Δ_k, and obtain

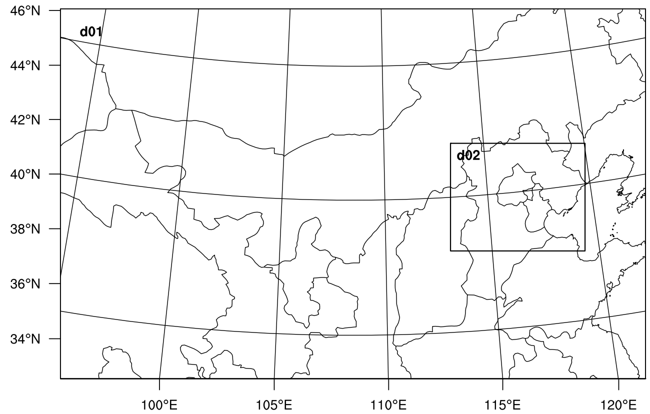

Figure 1. The two-grid horizontally nested domain with d01 being the outer grids and d02 being inner grids encompassing the Greater Beijing Area.

$X^2 = (x_1^0, \ldots, x_j^0 + \Delta_j, \ldots, x_k^0 + \Delta_k, \ldots, x_m^0)$. The gradient value $d_k^{(1)}$ from X^1 to X^2 is computed according to equation (1). This process is completed when all input variables are selected exactly once. Over a complete MOAT path, there are $m+1$ sampling points and m gradient values, $D^{(1)} = (d_1^{(1)}, d_2^{(1)}, \ldots, d_m^{(1)})$. Assuming that this procedure is repeated r times randomly, we have $(m+1) \times r$ sampling points in input space and r gradient values for each variable, i.e., $\boldsymbol{D} = (D^{(1)}, D^{(2)}, \ldots, D^{(r)})$. The following Morris measures [*Campolongo et al.*, 2007] can be computed:

$$u_j = \sum_{i=1}^{r} \left| d_j^{(i)} \right| / r \ \text{ and } \ \sigma_j = \sqrt{\sum_{i=1}^{r} \left(d_j^{(i)} - \sum_{i=1}^{r} d_j^{(i)} \Big/ r \right)^2 \Big/ r} \ , \ \ j = 1, 2, \ldots, m \qquad (2)$$

where u_j is the mean of $|d_j(i)|$ and σ_j is the standard deviation of d_j for the jth input variable. A large u_j indicates that x_j has the most influence on the output, whereas a large σ_j indicates that x_j has a strong nonlinear interaction with other input variables on the output. The MOAT method can identify sensitive parameters from insensitive parameters with a relatively small sample size [*Herman et al.*, 2013]. This is the reason we used it for studying the parametric uncertainty of the WRF model.

3. Experimental Design

3.1. WRF Model Configuration and Adjustable Parameters

The Advanced Research Weather Research and Forecasting model Version 3.3 (WRF-ARW Version 3.3, http://www.mmm.ucar.edu/wrf/users/) is used in this study. The study area is a two-grid horizontally nested domain with North China represented by the outer grids (i.e., d01 area in Figure 1) and the Greater Beijing Area (~24,300 km^2) by the inner grids (i.e., d02 area in Figure 1). The outer grids are composed of 87 × 55 grid cells with a spatial resolution of 27 km, and the inner grids are made of 60 × 45 grid cells with a spatial resolution of 9 km. The vertical profile is represented by 38 sigma vertical levels from the land surface to 50 hPa level in the atmosphere. The uniform time step is 60 s. Meteorological data including wind, temperature, water vapor, pressure, and land surface state variables from the National Center for Environmental Prediction (NCEP) Reanalysis data, available at 1° × 1° horizontal resolution and 6 h interval, are used to generate the initial and lateral boundary conditions. In this study, we focus on the evaluation of the impact of parametric uncertainty on the 5 day precipitation forecasts over the Greater Beijing Area during the summer from 2008 to 2010.

The choice of the physical parameterization schemes follows the operational setup by Beijing Meteorological Bureau. The Monin-Obukhov scheme [*Dudhia et al.*, 2003] is adopted for surface layer parameterization. Cumulus and microphysics parameterizations adopt the Kain-Fritsch Eta scheme [*Kain*, 2004] and the WSM 6-class Graupel scheme [*Hong and Lim*, 2006], respectively. The RRTM scheme [*Mlawer et al.*, 1997] and the Dudhia scheme [*Dudhia*, 1989] are chosen as long wave radiation and short wave radiation schemes. The unified Noah land surface model scheme [*Chen and Dudhia*, 2001] and the Yonsei University (YSU) scheme [*Hong and Lim*, 2006] are chosen as land surface and the planetary boundary layer schemes.

We identified 23 adjustable parameters from all seven parameterization schemes that may have influence on precipitation forecasting. Note that it is highly possible that this list is incomplete, and other potentially important parameters may have been missed. The physical meanings and the ranges of these parameters are presented as Table S1 in the supporting information. The parameters and their ranges for cumulus schemes are determined based on literature [*Yang et al.*, 2012]. The parameters of the land surface scheme are based on parameter SA results for the community/common land model [*Hou et al.*, 2012; *Li et al.*, 2013]

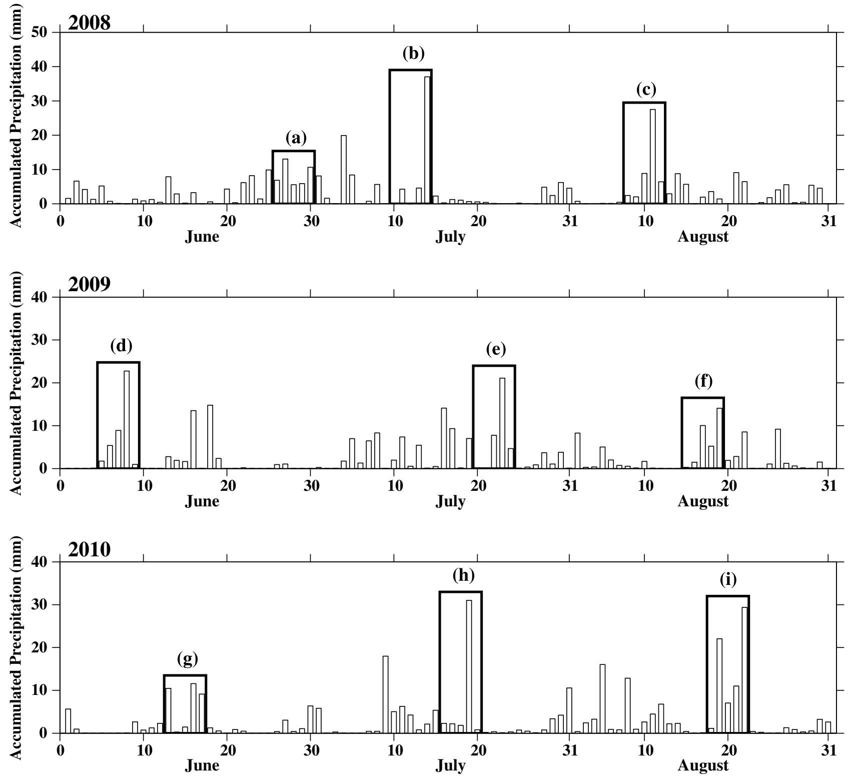

Figure 2. Daily precipitation of the Great Beijing Area for summer seasons from 2008 to 2010. Nine 5 day storms framed by the black boxes are indexed from (a) to (i).

and for the WRF model [*Xiong et al*., 2010]. The default values of the four adjustable parameters for the land surface scheme are specified according to the lookup tables based on the 17-category soil data set (Food and Agriculture Organization-State Soil Geographic). The values of these parameters are changed via multipliers applied to them, so they would change by the same relative amount across all grids. The parameters and their ranges of the YSU planetary boundary layer scheme are determined based on discussion with the YSU scheme developers (S.Y. Hong, personal communication, 2013). Parameters of other physical schemes are determined according to literature, expert discussion, and a careful examination of related program codes (e.g., surface layer scheme: *Zhang and Anthes* [1982] and *Stensrud* [2007, pp. 160–161]; microphysics scheme: [*Hong et al*., 2006]; short wave radiation scheme: WRF3.3 user guide, p. 5–54 and *Stephens* [1984]; long wave radiation scheme: [*Sheng et al*., 2003, pp. 104–105]).

3.2. The Precipitation Events and Observation Data Sets Used in the Study

We considered nine storm events (marked as events (a)–(i) in Figure 2) over summers from 2008 to 2010 in the Greater Beijing Area. Each event spans 5 days and contains the maximum daily rainfall event in each month. A complete WRF simulation of nine storm events consumes approximately 180 CPU hours.

The validation data are obtained from Beijing Normal University gridded precipitation data set [*Huang et al*., 2014]. The gridded precipitation data are available at 3 h interval with a spatial resolution of 0.05° × 0.05°. The cost function or performance measure is the mean absolute error (MAE) of daily rainfall simulation over the d02 domain:

$$\mathrm{MAE} = \frac{\sum_{t=1}^{T}\sum_{i=1}^{N}\left|\mathrm{sim}_i^t - \mathrm{obs}_i^t\right|}{N \times T}, \tag{3}$$

where sim_i^t and obs_i^t are simulated and observed daily precipitation at grid i and time t, N is the number of grid cells in domain d02, and T is the total number of days. The choice of performance measures is important when validating model performance [*Zepeda-Arce et al*., 2000; *Ebert and McBride*, 2000]. Since this paper

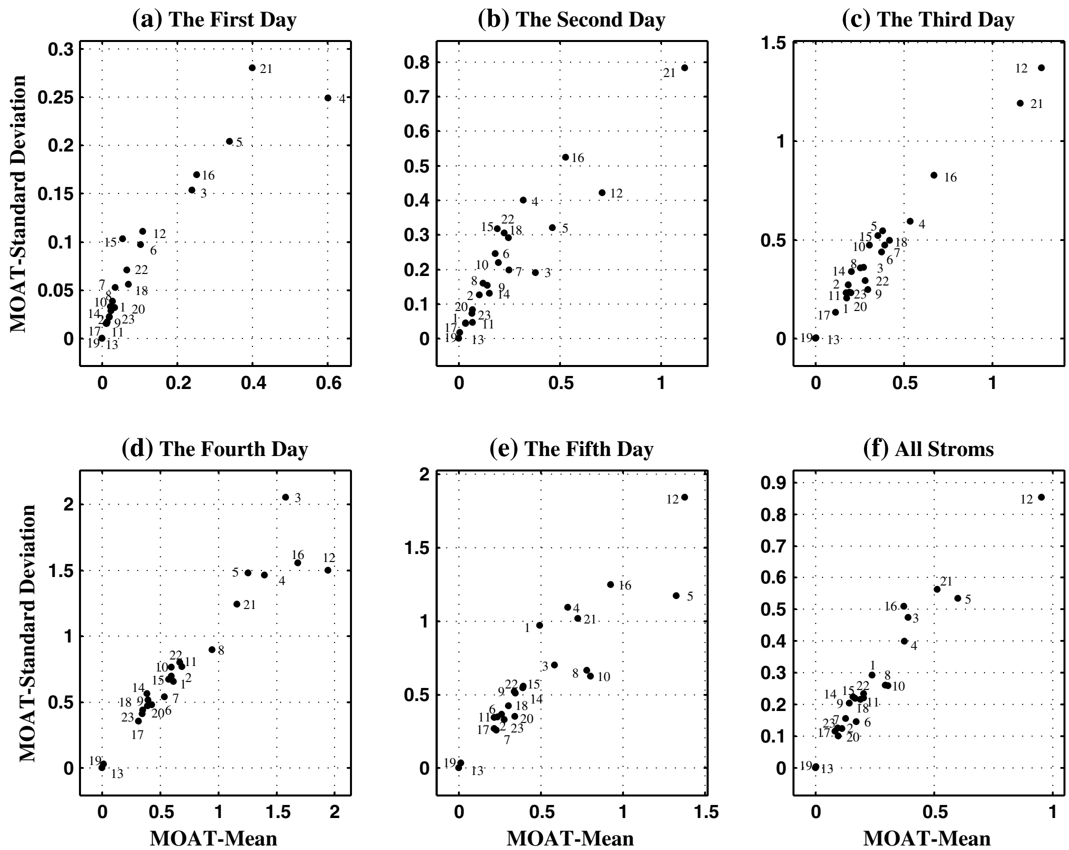

Figure 3. The MOAT sensitivity plots for different lead times: (a)–(e) Lead time from day 1 to day 5, respectively and (f) for all storms.

focuses on assessing the variation in model output due to different parameters, not on comparing model output and observation, MAE is a sufficient performance measure.

3.3. Experimental Setup for Sensitivity Analysis

We used the MOAT method to conduct SA, available from a software package named Problem Solving environment for Uncertainty Analysis and Design Exploration (PSUADE) [*Tong*, 2005]. PSUADE integrates many methods for uncertainty quantification, including a vast array of sampling, sensitivity analysis, surrogate model construction, and optimization methods. It has been successfully used in numerous studies [*Tong and Graziani*, 2008; *Li et al.*, 2013; *Gan et al.*, 2014].

Based on our previous experience with the MOAT method and literature [*Li et al.*, 2013; *Gan et al.*, 2014; *Morris*, 1991], we choose 10 MOAT replications to compute sensitivity indices. The total number of WRF simulations (i.e., parameter samples) is equal to $10 \times (23 + 1) = 240$, resulting in approximately $180 \times 240 = 43{,}200$ CPU hours to complete the analysis.

4. Results and Discussion

4.1. The Parameter Sensitivity Results Based on Lead Times

Using the experimental setup described before, we ran the WRF model using 240 randomly generated parameter sets based on the MOAT design. We then computed the MOAT indices for all storm events based on different lead times. Figures 3a–3e display the results for day 1 to day 5, while Figure 3f shows the result for all lead times considered together. In the figure, the larger the MOAT mean (horizontal axis), the more sensitive the parameter is. The MOAT standard deviation (vertical axis) is a reflection of nonlinear interaction among parameters, with the larger values implying higher interaction. The most sensitive parameters for day 1 are P3, P4, P5, P16, and P21. For days 2 and 3, many of the most sensitive parameters are in common

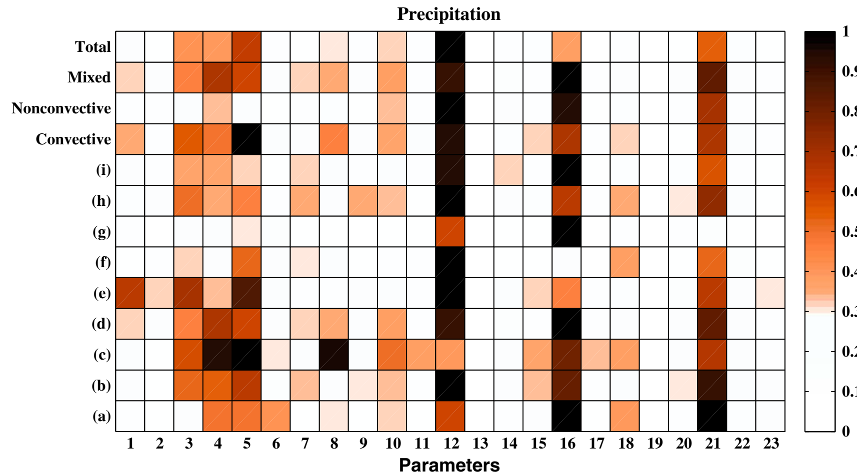

Figure 4. The normalized MOAT means for different storms, with 1 implying the most sensitive and 0 the least sensitive parameters.

with day 1 except for P5 in day 2 and P4 in day 3. For days 4 and 5, the most sensitive parameters are the same, except for P10, which appears only in day 5. When all lead times are considered together, the eight most sensitive parameters are basically the same as those identified based on individual lead times. Although there is some difference in the list of top sensitivity parameters, the sensitivity results seem to be independent of lead times.

4.2. The Parameter Sensitivity Results for Individual Storms and Different Storm Type

It is reasonable to hypothesize that the sensitivity of WRF model parameters is related to storm type. For example, some parameters may play a more prominent role in convective storms while others may have more influence on nonconvective storms. To test this hypothesis, we classify the nine storms into three categories according to the weight of simulated convective rainfall amount. A storm is classified as follows: (1) a convective storm if the simulated convective rainfall amount is >60%; (2) a nonconvective storm if the simulated convective rainfall is <40%; and (3) a mixed storm otherwise. Based on this rule, events (a), (c), (e), (f), and (g) (with 96%, 71%, 82%, 69%, and 91% convective rainfall, respectively) are regarded as convective, while events (b), (h), (i) (with 39%, 30%, and 37% convective rainfall) are nonconvective. Event (d) (with 49% convective rainfall) is a mixed storm.

For each storm type and individual storms, we computed the MOAT indices, which are exhibited in Figure 4. In order to gain insight into the relative parameter sensitivity, the MOAT mean values of all 23 parameters are normalized to [0, 1]. The sensitivity score for the most sensitive parameters is 1 (i.e., the darkest color), and 0 for the least sensitive (i.e., white).

For convective storms, the most sensitive parameters are P3, P4, P5, P8, P12, P16, and P21. For nonconvective storms, the most sensitive parameters are P4, P10, P12, P16, and P21. We note that the two storm types have many common sensitive parameters (e.g., P4, P12, P16, and P21). The combined list of parameters for the two storm type agrees with the most sensitive parameter list for all events and the list for the mixed storm. The difference among them is in the sensitivity ranks. For example, P3, P4, and P5, which belong to the cumulus scheme, are more sensitive in convective storms than in nonconvective storms. P12 (from shortwave scheme), P16 (from land surface scheme), and P21 (from planetary boundary layer scheme) are sensitive in almost all events. The sensitivity indices for individual storms tend to have more variation compared to that of their corresponding storm type, suggesting that sensitivity analysis results done with many storms are more robust than that with a single storm.

We also conducted an additional experiment to see if different initial and boundary conditions would change parameter sensitivities. Using the Climate Forecast System Reanalysis (CFSR) data set instead of the NCEP Reanalysis data set to initialize the WRF model, we performed SA for the 23 parameters using the MOAT method for the mixed storm event (i.e., event (d)). We found no difference in the list of sensitive parameters, even though the ranks do differ somewhat (see Figure S1 in supporting information), suggesting that parameter sensitivity is not dependent on how WRF is initialized.

4.3. The Physical Interpretation and Verification of the Parameter Sensitivity Results

Parameter P21, the profile shape exponent for calculating the momentum diffusivity coefficient in the planetary boundary layer (PBL), is one of the top-ranked sensitive parameters for precipitation simulation as it controls the mixing intensity of turbulent eddies in PBL and directly affect the development of convection. The sensitivity of P21 is confirmed by Aksoy et al. when they included it as part of parameter estimation [*Aksoy et al*., 2006]. Parameter P12, related to scattering in the clear sky from the short wave radiation scheme, also appears consistently as one of the top-ranked sensitive parameters as it directly influences the amount of simulated solar radiation reaching the ground, thus affects the amount of water vapor evaporated from the surface, and ultimately influences precipitation amount. This parameter must be tuned to compensate for the scheme not explicitly accounting for stratospheric ozone absorption [*Zamora et al*., 2005]. Two of the most sensitive parameters, P3 and P4 in the cumulus scheme, are related to downdraft and entrainment mass flux rates. Their inclusion is justified for the following reasons. A large value for P3 implies a large downdraft, which results in more evaporation from condensed water and consequently less precipitation. A large value for P4 indicates a strong entrainment rate, which dilutes the moist convective core, suppresses the updraft mass flux, and leads to less convective precipitation [*Kain and Fritsch*, 1990; *Kain*, 2004; *Yang et al*., 2012]. Another sensitive parameter P5 from the cumulus scheme, the downdraft starting height, has a similar effect on convection process as P3 because a downdraft flux initiating at a higher level would produce a tall and narrow downdraft to limit the development of convective precipitation. Two other parameters on the most sensitive parameter list, P8 and P10 from microphysics scheme, are the coefficient for solving the ice crystal fall velocity and the limited maximum value for the cloud ice diameter, respectively. Those two parameters, whose importance to precipitation is confirmed by *Jiang et al*. [2010], control the accretion amount from cloud ice to rain water. Soil porosity, P16 from the land surface scheme, is a sensitive parameter for precipitation simulation as it directly controls the transmission of water and heat fluxes in the soil, and the exchange of water vapor and heat between land surface and atmosphere [*Chen and Dudhia*, 2001].

To further verify if those results are reasonable, we computed parameter sensitivities using the traditional SA method, which works as follows: (1) perturb a specific parameter from its lower bound to upper bound with other parameters unchanged, (2) compute the change in MAE. The larger the change in MAE, the more sensitive is the parameter. Compared to the MOAT results, the parameter sensitivity ranks of traditional SA method is generally consistent, but some ranks are different (e.g., P4 and P16 are ranked 5 and 6 in MOAT, but 9 and 11 in traditional method, see Figure S2 in the supporting information). This result is reasonable because the difference in ranks can be explained by sampling error of the analysis methods. Our previous study has shown that traditional local SA method is more susceptible to sampling error than the MOAT method [*Li et al*., 2013]. Figure S3 in the supporting information shows the difference in mean daily rainfall over the nine 5 day forecasting period when selected parameters are perturbed from their lower bounds to upper bounds. The fact that the difference in rainfall due to perturbation of P4 and P16 is significant supports the argument that MOAT results are more reasonable than the traditional SA method.

5. Conclusions

In this study, we examined 23 WRF model parameters thought to have influence over precipitation amount and identified a subset of them as more sensitive than others for precipitation forecasting by using the MOAT method. The sensitivity was evaluated based on skill scores calculated over nine 5 day precipitation forecasts during summer from 2008 to 2010 in the Greater Beijing Area in North China. Two hundred forty randomly generated parameter sets based on the MOAT design were used to calculate parameter sensitivity. For convective storms, the most sensitive parameters are P3, P4, P5, P8, P12, P16, and P21. For nonconvective storms, the most sensitive parameters are P4, P10, P12, P16, and P21. These parameters come from physical schemes including microphysics, cumulus cloud, planetary boundary layer, land surface, and short wave radiation. The list of sensitive parameters is not dependent on storm type, but the sensitivity ranks do vary between storms, reflecting the fact that different storm-generating mechanisms dominate for different storm type. We examined the physical interpretations of the parameters on the most sensitive list and explained how these parameters influence precipitation simulation.

Parameter sensitivity is generally dependent on local conditions. Therefore, the results in the Greater Beijing Area may not hold true for other areas, especially those areas whose storm-generating mechanisms are different. To improve precipitation forecasting, we need to not only know what parameters are important but also know their optimal values. Our future work will focus on the optimization of WRF model parameters that are deemed sensitive.

Acknowledgments

We thank S.Y. Hong of Yonsei University, S. Miao and Y. Zhang of China Meteorological Administration, and Y. Dai and L. Chen of Beijing Normal University for their expert advice. Validation data are provided by X. Zheng (E-mail: x.zheng@bnu.edu.cn). We acknowledge NCEP Reanalysis data set obtained from http://rda.ucar.edu/datasets/ds083.2/ and the CFSR data set obtained from http://nomads.ncdc.noaa.gov/modeldata/. The research was partially supported by Beijing Excellent Talent Training Project (2012D009012000001), Fundamental Research Funds for the Central Universities of China (2012LYB40), and Natural Science Foundation of China (41305052&41375139). The work of Tong is performed under the auspices of the U.S. Department of Energy by Lawrence Livermore National Laboratory under contract DE-AC52-07NA27344.

Paul Williams thanks two anonymous reviewers for their assistance in evaluating this paper.

References

Aksoy, A., F. Zhang, and J. W. Nielsen-Gammon (2006), Ensemble-based simultaneous state and parameter estimation, *Geophys. Res. Lett.*, *33*, L12801, doi:10.1029/2006GL26186.

Bastidas, L. A., T. S. Hogue, S. Sorooshian, H. V. Gupta, and W. J. Shuttleworth (2006), Parameter sensitivity analysis for different complexity land surface models using multicriteria methods, *J. Geophys. Res.*, *111*, D20101, doi:10.1029/2005JD006377.

Bellprat, O., S. Kotlarski, D. Lüthi, and C. Schär (2012), Exploring perturbed physics ensembles in a regional climate model, *J. Clim.*, *25*, 4582–4599, doi:10.1175/JCLI-D-11-00275.1.

Bernardet, L. R., L. D. Grasso, J. E. Nachamkin, and C. A. Finley (2000), Simulating convective events using a high-resolution mesoscale model, *J. Geophys. Res.*, *105*(D11), 14,963–14,982, doi:10.1029/2000JD900100.

Campolongo, F., J. Cariboni, and A. Saltelli (2007), An effective screening design for sensitivity analysis of large models, *Environ. Model. Software*, *22*, 1509–1518, doi:10.1016/j.envsoft.2006.10.004.

Chen, F., and J. Dudhia (2001), Coupling an advanced land surface-hydrology model with the Penn State-NCAR MM5 modeling system. Part I: Model implementation and sensitivity, *Mon. Weather Rev.*, *129*, 569–585, doi:10.1175/1520-0493(2001)129<0587:CAALSH>2.0.CO;2.

Dudhia, J. (1989), Numerical study of convection observed during the winter monsoon experiment using a mesoscale two-dimensional model, *J. Atmos. Sci.*, *46*, 3077–3107, doi:10.1175/1520-0469(1989)046<3077:NSOCOD>2.0.CO;2.

Dudhia, J. (1993), A nonhydrostatic version of the Penn State-NCAR mesoscale model: Validation tests and simulation of an Atlantic cyclone and cold front, *Mon. Weather Rev.*, *121*, 1493–1513, doi:10.1175/1520-0493(1993)121<1493:ANVOTP>2.0.CO;2.

Dudhia, J. (2014), A history of mesoscale model development, *Asia-Pac. J. Atmos. Sci.*, *50*, 121–131, doi:10.1007/s13143-014-0031-8.

Dudhia, J., G. Dave, K. Manning, W. Wang, and C. Bruyere (2003), *PSU/NCAR Mesoscale Modeling System Tutorial Class Notes and User's Guide: MM5 Modeling System Version 3*, NCAR, Boulder, Colo.

Ebert, E., and J. L. McBride (2000), Verification of precipitation in weather systems: Determination of systematic errors, *J. Hydrol.*, *239*, 179–202, doi:10.1016/S0022-1694(00)00343-7.

Evensen, G. (1997), Advanced data assimilation in strongly nonlinear dynamics, *Mon. Weather Rev.*, *125*, 1342–1354, doi:10.1175/1520-0493 (1997)125<1342:ADAFSN>2.0.CO;2.

Gan, Y., Q. Duan, W. Gong, C. Tong, Y. Sun, W. Chu, A. Ye, C. Miao, and Z. Di (2014), A comprehensive evaluation of various sensitivity analysis methods: A case study with a hydrological model, *Environ. Model. Software*, *51*, 269–285, doi:10.1016/j.envsoft.2013.09.031.

Gilliam, R. C., and J. E. Pleim (2010), Performance assessment of new land surface and planetary boundary layer physics in the WRF-ARW, *J. Appl. Meteor. Climatol.*, *49*, 760–774, doi:10.1175/2009JAMC2126.1.

Grell, G. A., J. Dudhia, and D. R. Stauffer (1995), A description of the fifth-generation penn state/NCAR mesoscale model (MM5), *NCAR Technical Note, NCAR/TN-398 + STR*,122 pp., Natl. Cent. for Atmos. Res., Boulder, Colo.

Herman, J. D., J. B. Kollat, P. M. Reed, and T. Wagener (2013), Technical note: Method of Morris effectively reduces the computational demands of global sensitivity analysis for distributed watershed models, *Hydrol. Earth Syst. Sci.*, *17*, 2893–2903, doi:10.5194/hess-17-2893-2013.

Hong, S. Y., and J. O. J. Lim (2006), The WRF single-moment 6-class microphysics scheme (WSM6), *J. Korean Meteor. Soc.*, *42*, 129–151.

Hong, S. Y., J. Dudhia, and S. H. Chen (2004), A revised approach to ice microphysical processes for the bulk parameterization of clouds and precipitation, *Mon. Weather Rev.*, *132*, 103–120, doi:10.1175/1520-0493(2004)132<0103:ARATIM>2.0.CO;2.

Hong, S. Y., Y. Noh, and J. Dudhia (2006), A new vertical diffusion package with an explicit treatment of entrainment processes, *Mon. Weather Rev.*, *134*, 2318–2341, doi:10.1175/MWR3199.1.

Hou, Z., M. Huang, L. R. Leung, G. Lin, and D. M. Ricciuto (2012), Sensitivity of surface flux simulations to hydrologic parameters based on an uncertainty quantification framework applied to the Community Land Model, *J. Geophys. Res.*, *117*, D15108, doi:10.1029/2012JD017521.

Huang, C., X. Zheng, A. Tait, Y. Dai, C. Yang, Z. Chen, T. Li, and Z. Wang (2014), On using smoothing spline and residual correction to fuse rain gauge observations and remote sensing data, *J. Hydrol.*, *508*, 410–417, doi:10.1016/j.jhydrol.2013.11.022.

Huang, X., et al. (2009), Four-dimensional variational data assimilation for WRF: Formulation and preliminary results, *Mon. Weather Rev.*, *137*, 299–314, doi:10.1175/2008MWR2577.1.

Janjic, Z. I. (1994), The step-mountain eta coordinate model: Further developments of the convection, viscous sublayer, and turbulence closure schemes, *Mon. Weather Rev.*, *122*, 927–945, doi:10.1175/1520-0493(1994)122<0927:TSMECM>2.0.CO;2.

Jiang, H., G. Feingold, and A. Sorooshian (2010), Effect of aerosol on the susceptibility and efficiency of precipitation in warm trade cumulus clouds, *J. Atmos. Sci.*, *67*, 3525–3540, doi:10.1175/2010JAS3484.1.

Johannesson, G., D. Lucas, Y. Qian, L. P. Swile, and T. M. Wildey (2014), Sensitivity of precipitation to parameter values in the Community Atmosphere Model Version 5, Sandia Rep. SAND2014-0829, Sandia Natl. Lab., Albuquerque, N. M.

Kain, J. S. (2004), The Kain-Fritsch convective parameterization: An update, *J. Appl. Meteorol.*, *43*, 170–181, doi:10.1175/1520-0450(2004) 043<0170:TKCPAU>2.0.CO;2.

Kain, J. S., and J. M. Fritsch (1990), A one-dimensional entraining/detraining plume model and its application in convective parameterization, *J. Atmos. Sci.*, *47*, 2784–2802, doi:10.1175/1520-0469(1990)047<2784:AODEPM>2.0.CO;2.

Kalnay, E. (2003), *Atmospheric Modelling, Data Assimilation and Predictability*, Cambridge Univ. Press, U. K.

Kim, J. C., C. B. Lee, M. Belorid, and P. Zhao (2011), A study of sensitivity of WRF simulation to microphysics parameterizations, slope option and analysis nudging in Haean Basin, South Korea, Proceedings of 2011 TERRECO Science Conference, October 2 – 7, 2011; Karlsruhe Inst. of Tech., Garmisch-Partenkirchen, Germany.

Li, J., Q. Duan, W. Gong, A. Ye, Y. Dai, C. Miao, Z. Di, C. Tong, and Y. Sun (2013), Assessing parameter importance of the Common Land Model based on qualitative and quantitative sensitivity analysis, *Hydrol. Earth Syst. Sc.*, *10*, 2243–2286, doi:10.5194/hess-17-3279-2013.

Liang, X.-Z., et al. (2012), Regional Climate-Weather Research and Forecasting Model (CWRF), *Bull. Am. Meteorol. Soc.*, doi:10.1175/ BAMS-D-11-00180.1.

Liu, J., M. Bray, and D. Han (2013), Exploring the effect of data assimilation by WRF-3DVar for numerical rainfall prediction with different types of storm events, *Hydrol. Process.*, *27*, 3627–3640, doi:10.1002/hyp.9488.

Liu, Y., H. V. Gupta, S. Sorooshian, L. A. Bastidas, and W. J. Shuttleworth (2004), Exploring parameter sensitivities of the land surface using a locally coupled land-atmosphere model, *J. Geophys. Res.*, *109*, D21101, doi:10.1029/2004JD004730.

Mlawer, E. J., S. J. Taubman, P. D. Brown, and J. L. Lacono (1997), Radiative transfer for inhomogeneous atmospheres: RRTM, a validated correlated-k model for the longwave, *J. Geophys. Res.*, *102*, 16,663–16,682, doi:10.1029/97JD00237.

Morris, M. D. (1991), Factorial sampling plans for preliminary computational experiments, *Technometrics*, *33*, 161–174, doi:10.1080/00401706.1991.10484804.

Nasrollahi, N., A. Aghakouchak, J. Li, X. Gao, K. Hsu, and S. Sorooshian (2012), Assessing the impacts of different WRF precipitation physics in hurricane simulations, *Weather Forecasting*, *27*, 1003–1016, doi:10.1175/WAF-D-10-05000.1.

Rabier, F. (2005), Overview of global data assimilation developments in numerical weather -prediction centres, *Q. J. R. Meteorol. Soc.*, *131*, 3215–3233, doi:10.1256/qj.05.129.

Ruiz, J. J., L. Ferreira, and A. C. Saulo (2007), WRF-ARW sensitivity to different planetary boundary layer parameterization over South America,4-11 and 4-12 Research activities in atmospheric and oceanic modeling, in *WGNE Blue Book*, WMO, Geneva, Switzerland. [Available at http://collaboration.cmc.ec.gc.ca/science/wgne/BlueBook/index.html].

Saltelli, A., S. Tarantola, F. Campolongo, and M. Ratto (2004), *Sensitivity Analysis in Practice: A guide to Assessing Scientific Models*, John Wiley, New York.

Sheng, P., J. Miao, J. Li, A. Zhang, J. Sang, and N. Pan (2003), *Atmospheric Physics* [in Chinese], pp. 106–107, Beijing Univ. Press, Beijing.

Skamarock, W. C., J. B. Klemp, J. Dudhia, D. O. Gill, D. M. Barker, M. G. Duda, X. Huang, W. Wang, and J. G. Powers (2008), A description of the Advanced Research WRF Version 3, *NCAR Technical Note, NCAR/TN-475 + STR,* doi:10.5065/D68S4MVH.

Stensrud, D. J. (2007), *Parameterization Schemes: Keys to Understanding Numerical Weather Prediction Models*, Cambridge Univ. Press, Cambridge, U. K.

Stephens, G. L. (1984), The parameterization of radiation for numerical weather prediction and climate models, *Mon. Weather Rev.*, *112*, 826–867, doi:10.1175/1520-0493(1984)112<0826:TPORFN>2.0.CO;2.

Tong, C. (2005), *PSUADE User's Manual*, pp. 109–110, Lawrence Livermore Natl. Lab. (LLNL), Calif.

Tong, C., and F. Graziani (2008), Computational methods in transport: verification and validation, in *A Practical Global Sensitivity Analysis Methodology for Multi-Physics Applications*, pp. 277–299, Springer, Berlin.

Tripoli, G. J., and W. R. Cotton (1982), The Colorado State University three-dimensional cloud/mesoscale model-1982. Part I: General theoretical framework and sensitivity experiments, *J. de Rech. Atmos.*, *16*, 185–220.

Wang, X., D. M. Barker, C. Snyder, and T. M. Hamill (2008), A Hybrid ETKF–3DVAR data assimilation scheme for the WRF model. Part I: Observing system simulation experiment, *Mon. Weather Rev.*, *136*, 5116–5131, doi:10.1175/2008MWR2444.1.

Xiao, Q., and J. Sun (2007), Multiple radar data assimilation and short-range quantitative precipitation forecasting of a squall line observed during IHOP_2002, *Mon. Weather Rev.*, *135*, 3381–3404, doi:10.1175/MWR3471.1.

Xiong, S., X. Zeng, J. Liu, and Z. Wu (2010), Numerical simulation on the sensitivity of a heavy rain case to the random disturbances of land surface parameters, *Torrential Rain Disasters*, *29*, 117–121.

Yang, B., Y. Qian, G. Lin, R. Leung, and Y. Zhang (2012), Some issues in uncertainty quantification and parameter tuning: A case study of convective parameterization scheme in the WRF regional climate model, *Atmos. Chem. Phys.*, *12*, 2409–2427, doi:10.5194/acp-12-2409-2012.

Zamora, R. J., E. G. Dutton, M. Trainer, S. A. Mckeen, J. M. Wilczak, and Y. T. Hou (2005), The accuracy of solar irradiance calculations used in mesoscale numerical weather prediction, *Mon. Weather Rev.*, *133*, 783–792, doi:10.1175/MWR2886.1.

Zepeda-Arce, J., E. Foufoula-Georgiou, and K. K. Droegemeier (2000), Space-time rainfall organization and its role in validating quantitative precipitation forecasts, *J. Geophys. Res.*, *105*(D8), 10,129–10,146, doi:10.1029/1999JD901087.

Zhang, D., and A. R. Anthes (1982), A high-resolution model of the planetary boundary layer-sensitivity tests and comparisons with SESAME-79 data, *J. Appl. Meteorol.*, *21*, 1594–1609, doi:10.1175/1520-0450(1982)021<1594:AHRMOT>2.0.CO;2.